Experimental analysis of the vibroacoustic response of an electric window-lift gear motor generated by the contact between carbon brushes and commutator

S.Diop[1]

INTEVA Products, 14220 ESSON, France

Laboratoire de Tribologie et Dynamique des Systèmes, UMR CNRS 5513, Ecole Centrale de Lyon, Université de Lyon, 36 avenue Guy de Collongue, 69134 ECULLY cedex, France

sarah.diop@doctorant.ec-lyon.fr

E. Rigaud

Laboratoire de Tribologie et Dynamique des Systèmes, UMR CNRS 5513, Ecole Centrale de Lyon, Université de Lyon, 36 avenue Guy de Collongue, 69134 ECULLY cedex, France

emmanuel.rigaud@ec-lyon.fr

P-H. Cornuault

Univ. Bourgogne Franche-Comté, FEMTO-ST Institute, CNRS/UFC/ENSMM/UTBM, Department of Applied Mechanics, 25000 BESANÇON-FR, France

[1] Corresponding author.

pierre-henri.cornuault@ens2m.fr

E. Grandais-Menant

INTEVA Products, 14220 ESSON, France

EGrandaisMenant@intevaproducts.com

B. Bazin

INTEVA Products, 14220 ESSON, France

BBazin@intevaproducts.com

ABSTRACT

This paper deals with the vibroacoustic behavior of an electric window-lift gear motor for automotive vehicle which consists of a DC motor and a worm gear. After describing the overall vibroacoustic behavior of this system and identifying the various excitation sources involved, this study focuses on the excitation sources associated to the contacts between brushes and commutator. To that end, a specific test bench is designed. It makes use of a modified gear motor for which various specific rotors are driven with an external brushless motor. It allows the discrimination of some excitation sources associated to the contact between brushes and commutator by removing them one after the other. The respective weight of friction, mechanical shocks, electrical current flow and commutation arcs occurring jointly at the brush/commutator interface are dissociated and evaluated. The friction and the mechanical shocks between brushes and commutator blades increase the vibroacoustic response of the window-lift gear motor. The flowing of electrical current in brushes/commutator contacts tends to moderate the

frictional component of excitation sources while commutation arcs induce their rising, leading to a global additive contribution to the dynamic response.

Keywords: DC motor, vibroacoustic response, brush/commutator contact, friction noise, mechanical shocks, electrical current flow, commutation arcs.

1. INTRODUCTION

Like other performances offered by an automotive vehicle such as safety, dynamics and fuel economy, the acoustic comfort within the passenger compartment has to be considered closely in the design process. During last decades, efforts have been continuously made to significantly reduce noise emission of powertrain [1]. Consequently, nuisance coming from the vehicle motorized accessories have now a significant impact on the noise perceived inside the automotive interior [2]. Among these, a gear motor equips each door of newer automotive vehicles in order to allow driver to go up and down the window. The window-lift gear motor is one of these peripheral organs which may annoy and disturb the driver when it is often used at vehicle stop [3].

The window-lift gear motor studied herein consists of a DC motor and a worm gear (cf. Figure 1). Its housing is made of a steel stator which supports diametrically opposed ferrites generating a permanent magnetic field, and a plastic part which supports the cage containing two metal-graphitic brushes supplying electrical power to the rotor. The housing is attached to the door of the automotive vehicle at three fixation points. The rotor is guided by a front, a center and a rear journal bearings. It consists of a shaft on

which coils are wound (number of coils: N=10) and connected to the N blades of a rotating commutator. When the current flows in the coils positioned within the magnetic field, tangential (Lorentz) and radial (Maxwell) electromagnetic forces are created. The tangential forces generate the input torque allowing the rotating motion of the rotor. A worm is machined in the steel rotor, between the front and the center journal bearings. It is designed such as the meshing frequency f_m is equal to the rotor frequency f_r. It meshes with a polyoxymethylene (POM) helical gear wheel in order to reduce the rotation velocity and increase the output torque (number of gear teeth: Z=73, worm gear ratio 1:73). The axial component of the mesh force is taken up by two curved pads acting as axial stops and mounted at each of the rotor ends. Finally, the gear wheel goes up and down the window depending on the direction of rotation of the window-lift motor, via a mechanical clutch connected to a drum and cables mechanism. Under standard operating conditions, the motor operates in open loop mode. A constant voltage is applied (14.5 V). The rotor velocity first increases briefly until reaching almost 7000 rpm, then remains constant during approximately 4 seconds, and then decreases in a short time when the voltage is removed. Time evolution of the rotor velocity during the window motion is displayed in Figure 2a. The output torque is nearly equal to 3 N.m.

After manufacturing, assessment of the vibroacoustic behavior of some window-lift gear motors is usually conducted through a qualification test. For this purpose, a gear motor is attached to a rigid frame at the three fixation points. A 3 N.m torque is applied. A piezoelectric accelerometer is glued on the outer face of the plastic housing close to the brushes/commutator contacts (cf. Figure 1). It has been previously demonstrated that this accelerometer location allows for acquiring a signal level representative of the overall

gear motor vibroacoustic response. Measurements are performed using a slow increasing sweep (60 seconds) of the rotor velocity from 0 to V_t and a constant velocity regime longer than the standard operating duration (10 seconds), in order to qualify the vibroacoustic response of the gear motor. Time evolution of rotor velocity is shown in Figure 2b, with V_t = 7000 rpm. Vibroacoustic response is recorded using a data acquisition system with a sampling frequency equal to 44.1 kHz and post processing is performed in order to plot the spectrogram during the increasing sweep (see Figure 3b) and the power spectral density (PSD) during the constant regime (see Figure 3a).

At 7000 rpm, the RMS value of the acceleration response measured in the vicinity of the brushes/commutator contacts is of the order of 7 $m.s^{-2}$ that is 68 dB if the vibratory reference is taken at 10^{-6} $m.s^{-2}$. The Figure 3a highlights that the dynamic response shows many tonals corresponding to multiples of the rotation frequency f_r which are superimposed on a broadband noise, especially between 0 and 6 kHz. In this frequency range, the RMS value is 67 dB. The level of the dynamic response between 6 kHz and 20 kHz is lower and corresponds mainly to a broadband noise. In this frequency range, the RMS value is 55 dB. The highest peaks emerging from the broadband noise level correspond to harmonics H1, H10 and H20. To determine the weight of the RMS value due to the tonals, the following methodology is applied. First, the RMS value of the overall acceleration signal RMS_{total} is calculated. Second, rectangular windows centered on the successive harmonics H_i of the rotation frequency are applied in order to identify the tonal part of the total signal. For each harmonic H_i, the frequency range is defined as follows:

$$\Delta f = [f_i - 3.\log_{10}(f_i) \; ; \; f_i + 3.\log_{10}(f_i)]$$

The broadband noise part is defined as the signal energy recorded out of these intervals. Finally, the tonals proportion of the signal (TP) is defined as follows:

$TP = RMS_{tonal}^2 / RMS_{total}^2$ (with $RMS_{total}^2 = RMS_{tonal}^2 + RMS_{broadband}^2$)

Tests performed with 5 different window-lift gear motors result in similar PSDs shape and show that TP = 82.7 ±2.8 % in the frequency range [0-6 kHz]. Moreover, a significant dispersion of the vibratory response is observed from one gear motor to another. Depending on the rotor velocity, the standard deviation of the acceleration RMS value reaches a maximum of 3 dB. Among all the reasons which could explain this dispersion, we can note the difference in production and assembly of the gear motor components, particularly the gear wheel manufacturing errors and the assembly between plastic and steel housings, or/and the misalignment between the rotor shaft and the bearings. Another reason explaining the dispersion is temperature variation between tests. It must be noticed that tests duration are greater than the usual operating duration of the window-lift gear motor. Hence, temperature rise more than usual leading to modifications of the acceleration response due to various physical phenomena such as parts expansion, changes in the loads transmission, frictional behavior modification, etc. Indeed, preliminary tests performed with the same window-lift gear motor at different temperatures (measured on the steel housing) comprised between 23 and 39°C have shown a linear increase of 0.28 dB/°C of the acceleration RMS value at 4500 rpm. The Figure 3b confirms emergence of the H1, H10 and H20 harmonics. Two modal amplification areas are also observed around 1 kHz and 2.2 kHz.

The existence of broadband noise and tonals corresponding to multiples of the rotation frequency f_r (mainly H1, H10 and H20 harmonics) on both the PSD and the spectrogram is due to various mechanical and electromagnetic phenomena acting as excitation sources of the window-lift gear motor. The following excitation sources have been identified:

- The fluctuation of the input electrical current at the contact between commutator and brushes and the periodic motion of the rotating coils through the permanent magnetic field generate periodic fluctuation of radial and tangential electromagnetic forces. Fluctuation of the radial forces directly excites the steel housing of the stator [4]. Fluctuation of tangential forces and the corresponding input torque is transmitted to the stator through the worm gear helical contact, the journal bearings and the axial pads. The fundamental frequency characterizing the periodic fluctuation of tangential and radial forces is the harmonic H10.

- Shaft misalignment and mechanical imbalance induced by the asymmetry of the rotor are responsible for radial forces transmitted to the stator through the journal bearings and the axial pads [5, 6]. The fundamental frequency characterizing the periodic fluctuation of tangential and radial forces is the harmonic H1.

- The sliding contacts between worm and gear surfaces and between rotor/stator surfaces at the three journal bearings and the two axial pads generate friction noise [7]. The frictional noise due to sliding contacts generates broadband noise.

- The meshing between the worm and the gear wheel is the source of an internal excitation corresponding to the static transmission error (STE) fluctuation. STE corresponds to the difference between the actual position of the driven gear and its

theoretical one [8]. Its characteristics depend on the instantaneous locations of the meshing tooth pairs resulting from tooth deflections and manufacturing errors. Furthermore, the gear mesh stiffness fluctuation associated with STE generates a parametric excitation of the mechanical system [9]. Under operating conditions, the internal excitation due to the meshing process is the origin of dynamic gear loads which are transmitted to the stator via the gear wheel body, the rotor, the journal bearings and the axial pads [9]. The fundamental frequency characterizing the worm gear meshing is the harmonic H1, and sliding between contact surfaces generates broadband noise.

- At contacts between brushes and rotating commutator, (1) some mechanical shocks occur when brushes come into contact with the commutator blades, (2) the sliding contact between surfaces of the brushes and the commutator generates friction noise [7] and (3) commutation arcs occur when brushes lose contact with the blades [11]. The fundamental frequency characterizing the mechanical shocks is the harmonic H10. Sliding contacts generate broadband noise. The involvement of commutation arcs on the vibratory response is more complex. Commutation induces modification of sliding surface roughness by arcing and also contributes to broadband noise. Nevertheless, as commutation arcs occur at one edge of every commutator bars, it also contributes to the emergence of the fundamental frequency H10.

Among the excitation sources listed above, some of them can be assessed using numerical approaches. For example, Dupont [11] proposed a simulation methodology to calculate the noise of an electrical motor generated by the radial (Maxwell) electromagnetic forces applied to the stator. Hamzaoui et al. [12, 13] proposed to describe the vibroacoustic response of a rotor on bearings system taking account of misalignment

and imbalance. Concerning excitation sources generated by the meshing process, Tavakoli et al. [14] and Rigaud et al. [15] proposed a modeling of the gear teeth contact allowing evaluation of static transmission error and mesh stiffness periodic fluctuations. The methodology was then extended to the worm gear mesh [16, 17]. Prediction of the whining noise induced by these excitations was performed by Carbonelli [18]. Models of the overall dynamic response should also consider potential coupling between the different excitation sources. For this purpose, Dupont et al. [11] analyzed effect of static and dynamic rotor eccentricity on the radial magnetic excitation and the noise radiated by an automotive electric motor.

Nevertheless, others excitation sources such as those linked to the contacts between brushes and commutator are difficult to model, and an experimental approach seems more appropriated to analyze their contribution to the vibroacoustic response of the gear motor. Hence, this article presents an experimental approach for measuring the respective weight of electrical commutation arcs, mechanical shocks, electrical current flowing, and friction noise between brushes and commutator blades. The overall methodology adopted herein is inspired from the experimental works of Cameron et al [19] for eliminating progressively various sources in doubly salient variable-reluctance motors in order to identify the dominant noise source. The first part describes the specific test bench designed, as well as the protocol used. Different test configurations are chosen in order to characterize the vibroacoustic behavior of different gear motor modifications corresponding to the removal of the different excitation sources listed above one after the other. The results obtained in the successive configurations are then compared in a second part, to assess the relative weight of the studied excitation sources.

2. EXPERIMENTAL APPARATUS AND MEASUREMENT PROTOCOL

A test bench has been designed and built in order to analyze the separated influences of electrical current flow, commutation arcs, mechanical shocks and friction noise between brushes and commutator blades on the window-lift gear motor vibratory response. These steps involve removing some components essential to the gear motor operation. This leads to perform tests using a modified window-lift gear motor in which electromagnetic forces are removed by using steel housing equipped with demagnetized magnets. Hence, in the absence of Lorentz force, the rotor is driven by an external brushless motor fixed to the rigid frame, via flexible mechanical couplings, belt and pulleys guided in rotation by rolling bearings. In this configuration, the rotating velocity is limited to 4500 rpm. Moreover, modified rotors must be used. As mentioned above, friction, mechanical shocks, electrical current flow and commutation arcs occur jointly at the brush/commutator interface. Consequently, the three following prototypes are used in order to dissociate the effect of these excitation sources.

Rotor 1: the commutator is intentionally not segmented. This affects the brushes/commutator interaction by suppressing the mechanical shocks which usually occur when a brush rubs from a commutator blade to the following one. Moreover, coils are also electrically short-circuited, resulting in the lack of commutation arcs when electrical current flows through the brush/commutator contact.

Rotor 2: the commutator remains segmented but the electrical connections between coils and commutator blades are cut off. All blades have been connected together with a copper wire which has been soldered at each blade ending in order to allow electrical

current flowing from one brush to the second one through the commutator. Consequently, commutation arcs do not occur due to coils short-circuiting.

Rotor 3: this rotor is unchanged compared to the rotor used in a classical window-lift gear motor.

For each rotor, brushes can rub on the commutator or can be removed. In the case of brushes rubbing on the commutator, electrical current can be injected or not. The use of the 3 rotors combined with the existence (or not) of brushes and electrical current flow involves various test conditions for which friction, mechanical shocks, electrical current flow and commutation arcs can be independently applied or removed. The Table 1 lists the testing conditions which were used for the 7 trials named A to G. Five tests were performed for each trial.

As depicted in Figure 4, the modified gear motor is mounted on a rigid and compact frame at the three points corresponding to its fixation points to the door of the automotive vehicle. An output shaft driven by the gear wheel is connected to a magnetic powder brake thanks to a flexible mechanical coupling. The kinematic chain is guided in rotation by rolling bearings. The powder brake applies the load which is usually required to translate the window. This one is measured using a torque meter. The output gear motor rotation velocity is measured using a speed meter fixed to the end of the output shaft. The test bench is controlled using a specific software. Tests are performed for an output torque equal to 3 N.m and following the rotor velocity evolution described in Figure 1b, with V_t = 4500 rpm. Vibratory response is measured using a piezoelectric accelerometer glued at the reference point corresponding to the standard qualification test. The

accelerometer sensitivity and weight are respectively 10.27 $mV/m.s^{-2}$ and 4 g. Acoustic response is measured using a 1/4 inch microphone placed close to the brushes/commutator contacts. Time evolution of signals is recorded using a multi channels acquisition card. The sampling frequency is 44.1 kHz. The acoustic and vibratory references are respectively 2.10^{-5} Pa and 1.10^{-6} $m.s^{-2}$. Then, signals are post processed in order to analyze their PSD, spectrogram, and the corresponding evolution of the RMS value versus operating velocity.

3. EXPERIMENTAL RESULTS AND DISCUSSION

Every trial leads to plot the evolution of the mean RMS value of the vibroacoustic response versus the rotor velocity resulting in a curve similar to Figure 5 which corresponds to trial C. The length of vertical bars represents the standard deviation measured for the five tests of a single trial. Instead of the use of the same prototype, one notes a similar dispersion than the one observed for the standard gear motor. Moreover, Figure 5 highlights a significant increase of the vibroacoustic response versus rotor velocity. Assuming a linear increase of the RMS value (in dB) versus the logarithm of the rotor velocity, a linear approximation is plotted for each trial. The mean slope of these fits is 7.4 ±1.0 dB/octave. The value of the linear fit at 4500 rpm for each trial is reported in Table 1.

The results interpretation methodology has to take account for gear motor vibroacoustic response dispersion related to components assembly and rotors design even if the difference of shape and mass between the three prototypes is weak. Indeed, the standard deviation of the RMS values for trials A, C and F is ±0.9 dB whereas test conditions are

the same, apart from the use of three different prototypes. Moreover, trials using the same prototype must be performed without any dismounting/assembly operation in order to avoid the measurements dispersion due to changes in rotor positioning, as previously mentioned. Consequently, the effect of the four excitation sources on the vibroacoustic behavior is quantified with respect to a reference setup. This one corresponds to the trials A, C and F. It means the reference vibroacoustic response is not the standard gear motor response, but is defined in the absence of brushes and electromagnetic forces. The cumulative effects of the four excitation sources are then considered by comparison of two trials for which the same prototype has been used without any dismounting.

The comparison between trials A and B shows an increase of 0.85 dB of the RMS value. As expected, this means that the addition of the brushes/commutator friction with respect to the reference setup increases the vibroacoustic response of the window-lift gear motor. The comparison of trials C and D shows an increase of 1.75 dB of the RMS value with respect to the reference setup. Thus, the mechanical shocks of brushes on the commutator blades edge involve an additional increase of the RMS value compared with the increase due to friction only. The comparison of trials C and E shows an increase of 1.1 dB when friction, mechanical shocks and electrical current flowing occur simultaneously at the brushes/commutator interfaces, with respect to the reference setup. An important feature of this result is the least increasing of the window-lift gear motor vibroacoustic response when electrical current flows through the contacts than without current (+1.1 dB against +1.75 dB). This result can be explained by the so-called “electro-lubrication” mechanism [20] which was first observed by Lancaster [21]. The friction force decrease with electrical current has been extensively observed [22-25] and explained by the

modification of graphitic platelets orientation on brushes surfaces due to electrostatic stress [21]. Zaidi et al. [25] carried out experiments with very similar testing conditions than those encountered in this paper in terms of normal load, velocity, materials, etc. They measured a decrease of approximately 30% of the friction coefficient when current flows through the contact. The flowing of electrical current in brushes/commutator contacts of the gear motor studied tends thus to moderate friction forces, resulting in the lowering of the excitation due to friction. The comparison of trials F and G shows a large increase of +2.2 dB of the RMS value when commutation occurs in addition to the three earlier excitation sources. Compared to the other trials, trial G highlights the major role played by commutation in the vibroacoustic behavior of the brushes/commutator system. Commutation phenomenon is usually associated to the presence of arcing and sparking at the brush/commutator contact [10]. These electrical discharges generate wear [26-28] which modifies the brushes and commutator surfaces topography and roughness and then induces an increase of friction forces [20, 29-30]. In the present study, surface damages owed by commutation arcs induce the rising of the frictional component of excitation sources.

Finally, the vibroacoustic response of the gear motor appears to be highly influenced by both friction and shocks occurring between the brushes and the commutator. In the case of friction, commutation tends to largely increase the acceleration response whereas electrical current flow leads to lowering it. Furthermore, similar trends are observed concerning the acoustical response measured with the microphone that is: +0.3 dB (compared with the reference setup) when only friction and shocks occur, +0.2 dB with the addition of electrical current, and +1.1 dB when commutation is added.

4. CONCLUSION

The experimental vibroacoustic behavior of an electric window-lift gear motor for automotive vehicle which consists of a DC motor and a worm gear has been studied. Standard qualification tests show that it is characterized by the dual existence of broadband noise and tonals corresponding to multiples of the rotation frequency. The tonal proportion of the signals is almost 80 % in the frequency rang [0-6 kHz]. Moreover, tests highlight the dispersion of results due to manufacturing uncertainties, components assembly, and operating temperature (+0.28 dB/°C).

After identifying the different excitation sources inducing the overall vibroacoustic response, this study has focused on the sources taking place at the brushes/commutator interfaces. These sources are: friction noise, mechanical shocks, electrical current flow and commutation arcs. For this purpose, a specific test bench has been designed and various specific prototypes driven with an external brushless motor have been used. Excitation sources have been discriminated by removing them one after the other. The respective weight of friction, mechanical shocks, electrical current flow and commutation arcs occurring jointly at the brush/commutator interface have been evaluated by overcoming the dispersion due to the components assembly and the design of different rotors used. The friction alone and the mechanical shocks between brushes and commutator blades increase the vibroacoustic response of the window-lift gear motor. The flowing of electrical current in brushes/commutator contacts tends to moderate component of excitation sources while commutation arcs induce their rising, leading to a global additive contribution to the dynamic response.

ACKNOWLEDGMENTS

The authors wish to thank M. Guibert, S. Zara, T. Durand and L. Charles for their contribution to the experimental apparatus development. The authors thank the LabCom LADAGE (Laboratoire de Dynamique des engrenAGEs) sponsored by the program ANR-14-LAB6-0003 and the Labex CeLyA (Centre Acoustique Lyonnais).

REFERENCES

[1] Qatu, M. S., Abdelhamid, M. K., Pang, J., and Sheng, G., 2009, "Overview of automotive noise and vibration," International Journal of Vehicle Noise and Vibration, 5(1-2), pp. 1–35, doi: 10.1504/IJVNV.2009.029187.

[2] Robinson, I., Walsh, S. J., and Stimpson, G., 1998, "Vehicle accessory tonal noise: experimental determination and subjective assessment," IN: Goodwin, V.C. and Stevenson, D.C. (eds.), Inter-noise 98: proceedings: the 1998 International Congress on Noise Control Engineering: Christchurch, New Zealand, 16-18 November 1998: sound and silence, setting the balance, Auckland, N.Z., New Zealand Acoustical Society, pp. 1049-1052.

[3] Revel, G. M., Santolhi, C., Tomasini, E. P, 1997, "Laser-dopler vibration and acoustic intensity measurements for dynamic characterization and noise reduction in a car window lift system," Proc. SPIE Vol. 3089, Proceedings of the 15th International Modal Analysis Conference, p. 1636.

[4] Hallal, J., Druesne, F., Lanfranchi, V., 2013, "Study of electromagnetic forces computation methods for machine vibration estimation," ISEF.

[5] Xut, M., Marangoni, R. D., 1994, "Vibration analysis of a motor-flexible coupling-rotor system subject to misalignment and unbalance. Part 1: Theoritical model analysis," Journal of sound and vibration, 176(5), pp. 663-679.

[6] Xut, M., Marangoni, R. D, 1994, “Vibration analysis of a motor-flexible coupling-rotor system subject to misalignment and unbalance. Part 2: Experimental validation,” Journal of sound and vibration 176(5), pp. 681-691.

[7] Le Bot, A., Bou Chakra, E., 2010, “Measurement of Friction Noise Versus Contact Area of Rough Surfaces Weakly Loaded,” Tribology Letters, 37(2), pp. 273-281.

[8] Welbourn, D. B., 1979, “Fundamental Knowledge of Gear Noise - A Survey,” Conference on Noise and Vibrations of Engines and Transmissions, Cranfield Institute of Technology, Paper C177/79, pp. 9-29.

[9] Rigaud, E., Sabot, J., Perret-Liaudet, J., 2000, “Comprehensive approach for the vibrational response analysis of a gearbox,” Revue européenne des éléments finis, 9(1-3), pp. 315-330.

[10] Holm, R., 1967, *Electric contacts - Theory and application*, Springer-Verlag, Berlin.

[11] Dupont, J. B., Aydoun, R., Bouvet, P., 2014, “Simulation of the Noise Radiated by an Automotive Electric Motor: Influence of the Motor Defects,” SAE International Journal of Alternative Powertrains, 3(2), pp. 310-320, doi: 10.4271/2014-01-2070.

[12] Hamzaoui, N., Boisson, C., Lesueur, C., 1998, “Vibroacoustic analysis and identification of defects in rotating machinery, part I: theoretical model,” Journal of sound and vibration, 216(4), pp. 553-570.

[13] Hamzaoui, N., Boisson, C., Lesueur, C., 1998, “Vibroacoustic analysis and identification of defects in rotating machinery, part II: experimental study,” Journal of sound and vibration, 216(4), pp. 571-583.

[14] Tavakoli, M. S., Houser, D. R., 1986, “Optimum Profile Modifications for the Minimization of Static Transmission Errors of Spur Gears,” J. Mech. Trans. and Automation, 108(1), pp. 86-94.

[15] Rigaud, E., Barday, D., 1999, “Modelling and analysis of static transmission error. Effect of wheel body deformation and interactions between adjacent loaded teeth,” 4th World Congress on Gearing and Power Transmission, Paris.

[16] Hiltcher, Y., Guingand, M., De Vaujany, J. P., 2006, “Load sharing of worm gear with a plastic wheel,” J Mech Design, 129(1), pp. 23-30, doi:10.1115/1.2359469.

[17] Jbily, D., Guingand, M., De Vaujany, J. P., 2014, “Loaded behaviour of steel/bronze worm gear,” International Gear Conference 2014 proceedings, pp. 32-42, Lyon (France).

[18] Carbonelli, A., Rigaud, E., Perret-Liaudet, J., 2016, “Vibro-Acoustic Analysis of Geared Systems—Predicting and Controlling the Whining Noise,” Automotive NVH Technology, pp. 63-79, Editors Fuchs A., Nijman E., Priebsch H-H., SpringerBriefs in Applied Sciences and Technology, Springer International Publishing. ISBN 978-3-319-24055-8.

[19] Cameron, D. E., Lang, J. H., 1992, “The origin and reduction of acoustic noise in doubly salient variable-reluctance motors,” IEEE Transactions on industry applications, 28(6).

[20] Braunovic, M., Konchitz, V. V., 2007, Myskkin N. K., *Electrical Contacts – Fundamentals Application & Technology*, CRC Press ed., London.

[21] Lancaster, J.K., 1964, "The effect of current on the friction of carbon brush materials," British Journal of Applied Physics, 15, pp. 29-43.

[22] Paulmier, D., El Mansori, M., Zaidi, H., 1997, "Study of magnetized or electrical sliding contact of a steel XC48/graphite couple," Wear, 203-204, pp. 148-154.

[23] Zhao, H., Barber, G. C., Liu, J., 2001, "Friction and wear in high speed sliding with and without electrical current," Wear, 248, pp. 409-414.

[24] Robert, F., Csapo, E., Zaidi, H., Paulmier, D., 1995, "Influence of the current and environment on the superficial structure of a graphite electrical collector," International Journal of Machine Tools & Manufacture, 35(2), pp. 259-262.

[25] Csapo, E., Zaidi, H., Paulmier, D., Kadiri, E. K., Bouchoucha, A., Robert, F., 1995, "Influence of the electrical current on the graphite surface in an electrical sliding contact," Surface and Coatings Technology, 76-77, pp. 421-424.

[26] Hamilton, R. J., 2000, "DC motor brush life," IEEE Transactions on industry applications, 36(6), pp. 1682-1687.

[27] Lawson, D. K., Dow, T. A., 1985, "The sparking and wear of high current density electrical current," Wear, 102, pp. 105-125.

[28] Sawa, K., Shimoda, N., 1992, “A study of commutation arcs of DC motors for automotive fuel-pumps,” IEEE Transactions on components, hybrids and manufacturing technology, 15(2), pp. 193-197.

[29] Shobert, E. I., 1965, *Carbon brushes – The physics and chemistry of sliding contact*, Chemical Publishing Company ed., New-York.

[30] Takaoka, M., Sawa, K., 2001, “An influence of commutation arcs in gasoline on brush wear and commutator,” IEEE Transactions on components and packaging technologies, 24(3), pp. 349-352.

TABLES CAPTIONS LIST

Table 1:

Test conditions of the trials A to G, excitation sources involved, and corresponding acceleration RMS values at 4500 rpm. $\ddot{x}$ is the acceleration, $\ddot{x}_{dB}$ is the value in dB (with reference 1.10^{-6} m/s²), and $\Delta\ddot{x}_{dB}$ is the difference in dB relative to reference trial (performed with the same prototype).

FIGURES CAPTIONS LIST

Fig. 1:

Window-lift gear motor. Steel (1) and plastic housings (11) – permanent magnet (2) – carbon brushes (6) – rear (4), center (7) and front bearings (9) – fixation points (12) – coils (3) – commutator (5) – worm (8) – gear wheel (10).

Fig. 2:

Time evolution of the rotor velocity. Standard operating conditions of the window-lift gear motor (a) Qualification test with V_t = 7000 rpm or trials with V_t = 4500 rpm (b).

Fig. 3:

Power spectrum density (PSD) at 7000 rpm (a) and spectrogram (b) of the vibroacoustic response.

Fig. 4:

Experimental test bench. Speed meter (1) - Torque meter (2) - Powder brake (3) - Flexible mechanical couplings (4) – External brushless motor (5).

Fig. 5:

Evolution of the acceleration RMS value versus rotor velocity for trial C. Red crosses are mean values. Vertical red bars are standard deviation. Blue dotted line is a linear approximation of RMS values versus rotor velocity.

Table 1:

Rotor	Trial	Brushes	Current flow	Excitation sources involved				$\ddot{x}$ RMS [m/s²]	$\ddot{x}_{dB}$ RMS [dB]	$\Delta\ddot{x}_{dB}$ RMS [dB]
				Friction	Shocks	Current	Arcs			
1	A	no	no					2.11	63.3	-
	B	yes	no	⊕				2.57	64.1	0.85
2	C	no	no					1.51	61.8	-
	D	yes	no	⊕	⊕			2.26	63.6	1.75
	E	yes	yes	⊕	⊕	⊕		1.95	62.9	1.10
3	F	no	no					2.19	63.4	-
	G	yes	yes	⊕	⊕	⊕	⊕	3.63	65.6	2.20

Figure 1

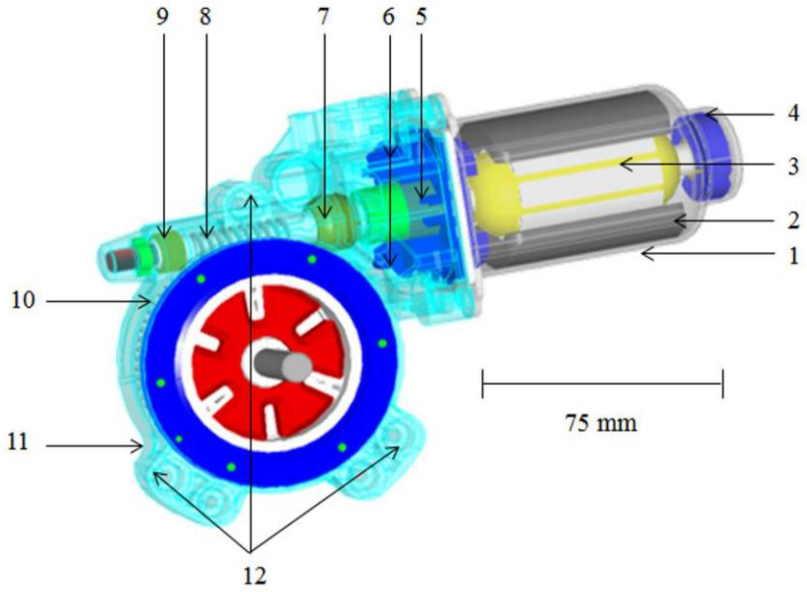

Figure 2

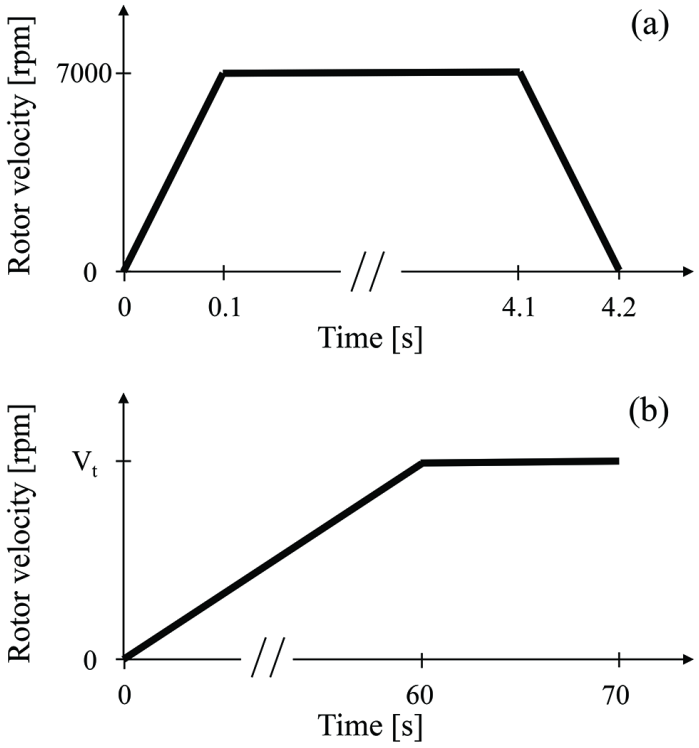
(a)
Rotor velocity [rpm]
7000
0
0
0.1
4.1
4.2
Time [s]
(b)
Rotor velocity [rpm]
V_t
0
0
60
70
Time [s]

Figure 3

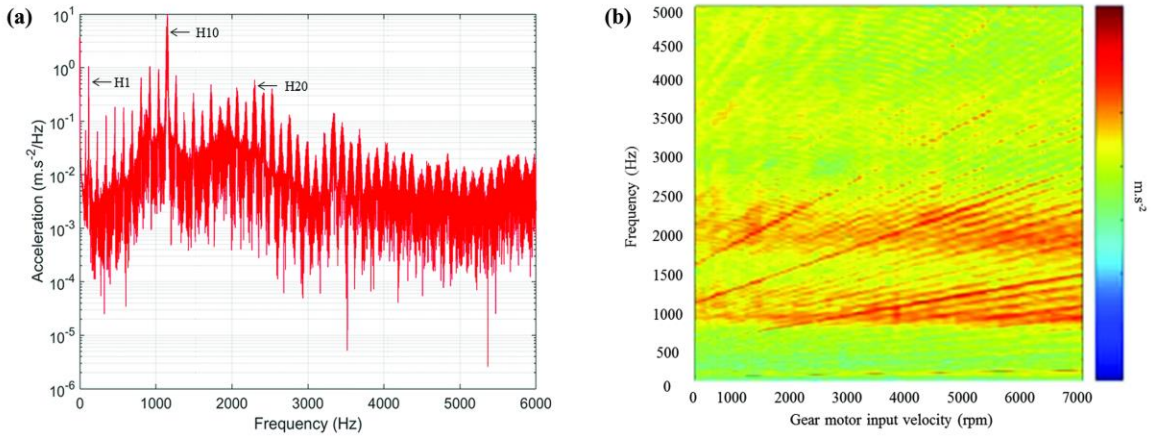
(a)
H10
H1
H20
Acceleration (m.s-2/Hz)
Frequency (Hz)
(b)
Frequency (Hz)
Gear motor input velocity (rpm)
m.s-2

Figure 4

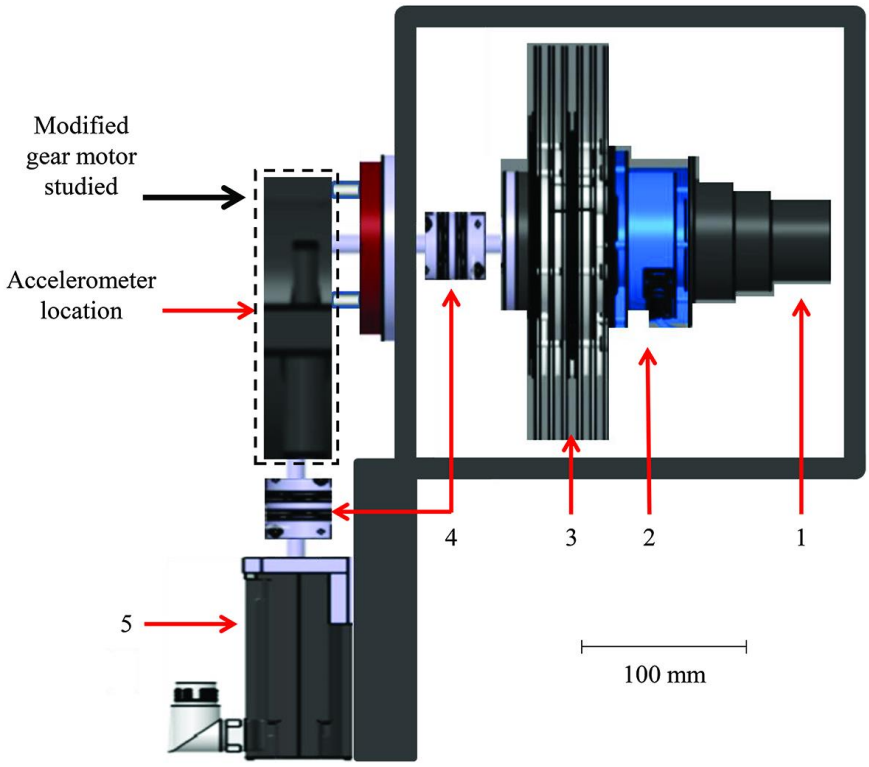
Modified
gear motor
studied
Accelerometer
location
4
3
2
1
5
100 mm

Figure 5

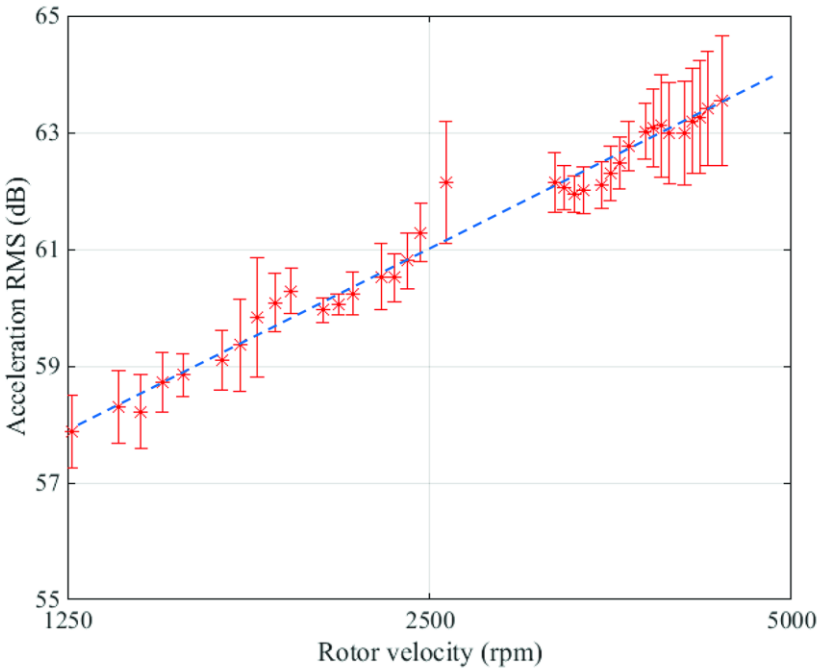
65
63
61
59
57
55
Acceleration RMS (dB)
1250
2500
5000
Rotor velocity (rpm)